

4-1-2003

# Spectroscopic Abundances of Solar-Type Dwarfs in the Open Cluster M34 (NGC 1039)

Simon C. Schuler  
*Clemson University*

Jeremy R. King  
*Clemson University, jking2@clemson.edu*

Debra A. Fischer  
*University of California*

David R. Soderblom  
*Space Telescope Science Institute*

Burton F. Jones  
*University of California*

Follow this and additional works at: [https://tigerprints.clemson.edu/physastro\\_pubs](https://tigerprints.clemson.edu/physastro_pubs)

---

## Recommended Citation

Please use publisher's recommended citation.

This Article is brought to you for free and open access by the Physics and Astronomy at TigerPrints. It has been accepted for inclusion in Publications by an authorized administrator of TigerPrints. For more information, please contact [kokeefe@clemson.edu](mailto:kokeefe@clemson.edu).

## SPECTROSCOPIC ABUNDANCES OF SOLAR-TYPE DWARFS IN THE OPEN CLUSTER M34 (NGC 1039)

SIMON C. SCHULER AND JEREMY R. KING

Department of Physics, University of Nevada, Las Vegas, 4505 Maryland Parkway, Las Vegas, NV 89154-4002;  
schuler@physics.unlv.edu, jking@physics.unlv.edu

DEBRA A. FISCHER

Department of Astronomy, 601 Campbell Hall, University of California at Berkeley, Berkeley, CA 94720-3411;  
fischer@serpens.berkeley.edu

DAVID R. SODERBLOM

Space Telescope Science Institute, 3700 San Martin Drive, Baltimore, MD 21218-2410; soderblom@stsci.edu

AND

BURTON F. JONES

UCO/Lick Observatory, Department of Astronomy and Astrophysics, University of California, Santa Cruz,  
1156 High Street, Santa Cruz, CA 95064-1077; jones@ucolick.org

Received 2002 September 9; accepted 2003 January 14

### ABSTRACT

Parameters and relative abundances of Fe, Ni, Ti, Cr, Ca, Si, Al, and Mg have been derived for nine M34 G and K dwarfs from high-resolution, modest signal-to-noise ratio Keck HIRES spectra. Effective temperatures have been derived spectroscopically and fall in the range  $4750 \text{ K} \leq T_{\text{eff}} \leq 6130 \text{ K}$ . Despite modest scatter in Fe, Ti, Cr, Ca, Al, and Mg (none of which is found to be correlated with Li scatter in M34), our two coolest stars are slightly though consistently underabundant in these elements relative to the warmer stars. The two cool stars are slightly overabundant in Si, whose abundances are derived from higher excitation lines. This and our finding that Fe II-based abundances are significantly higher than Fe I-based values in the cool stars seem to point toward the action of non-LTE effects (overionization, overexcitation, or both), though additional analysis is required to exclude inadequacies in the model atmospheres. Final mean cluster abundances are based on five warm stars, which indicate  $[\text{Fe}/\text{H}] = +0.07 \pm 0.04$ , and are void of any statistically significant scatter. The other elements scale well with Fe except for Ni, which appears to be slightly underabundant with respect to Fe. Potassium abundances are derived and show a surprising marked trend with temperature, which further supports our suspicion of the presence of non-LTE effects. Moreover, similar trends with temperature suggest that the Li and K underabundances in cool M34 dwarfs are partially related; thus, some portion of the well-known Li- $T_{\text{eff}}$  trend in cool M34 dwarfs may be illusory.

*Key words:* open clusters and associations: individual (M34 = NGC 1039) — stars: abundances — stars: atmospheres

*On-line material:* machine-readable table

### 1. INTRODUCTION

Open clusters and the elemental abundances of member stars have long been known to be of great astrophysical importance. Assuming they are of the same age and formed from a chemically homogeneous gas cloud, open cluster stars can serve as test beds for our understanding of stellar properties, which is then incorporated into our stellar models. However, it is apparent that stellar models in their standard form—those not including rotational mixing, magnetic fields, mass loss, or gravitational settling—are incomplete. Evidence of this is copious. For example, the observed Li spread in low-mass ( $M \leq 0.9 M_{\odot}$ ) G and K dwarfs in several open clusters—particularly in the Pleiades (Duncan & Jones 1983; Soderblom et al. 1993)—cannot be reproduced by standard models, but it has been shown that models including microscopic diffusion and rotational mixing might naturally produce such Li scatter (Chaboyer, Demarque, & Pinsonneault 1995). However, Chaboyer et al. (1995) also point out the importance of metallicity ( $[\text{Fe}/\text{H}]$ ) to the models. Scaling the relative Fe abundance while still assuming a solar mixture (and using the relation  $\Delta Y/\Delta Z = 2.5$  for the helium mass fraction) produced con-

siderable changes in their standard-model Li depletion predictions for Pleiades stars with effective temperature  $T_{\text{eff}} < 6000 \text{ K}$ :  $\Delta[\text{Fe}/\text{H}] = 0.05$  dex resulted in a change of  $\sim 0.4$  dex in the predicted Li abundance at  $T_{\text{eff}} = 5000 \text{ K}$ . In addition, Piau & Turck-Chièze (2002) have investigated the effects of altering metallicity and chemical composition on their model Li abundance predictions. They compared models using observed metallicities with models that used the lowest metallicity and highest helium mass fraction allowed within observational errors for both the Pleiades and the Hyades. Specifically, for the Pleiades varying the metallicity from  $-0.034$  to  $-0.058$  dex—corresponding to the mean  $[\text{Fe}/\text{H}]$  and the lower uncertainty of Boesgaard & Friel (1990)—and altering  $Y$  according to  $\Delta Y/\Delta Z = 3$  (Fernandes et al. 1998) produced a positive change of 0.35 dex in the Li abundance (for  $T_{\text{eff}} \sim 5800 \text{ K}$ ). Piau & Turck-Chièze also studied more detailed opacity effects on Li depletion, finding that a 1.7 dex ( $\sim 50$  times) increase in Li abundance resulted when the oxygen abundance within a Hyades model was changed from 0.127 (scaled to  $[\text{Fe}/\text{H}]$ ) to  $-0.07$  dex (observed  $[\text{O}/\text{H}]$  from García López et al. 1993) and the rest of the metals (except the iron-peak elements) were scaled with oxygen.

Interestingly, the ever increasing number of extrasolar planets being discovered may provide a mechanism by which intracluster abundance scatter could arise. Spectroscopic studies have shown enhanced metallicities relative to nearby field stars for stars with planets (e.g., Gonzalez et al. 2001). Accretion of high- $Z$  protoplanetary material onto the parent star has been suggested as a possible cause of abundance scatter. However, an alternate explanation for the increased metallicity might be that planetary systems prefer high-metallicity environments. Data exist supporting both hypotheses, making accurate *cluster* abundance calculations significant to clarifying the situation.

The importance of opacities has also been exhibited in comparing stellar models and observations of the overall level of Li depletion in cool stars in open clusters of differing age. Swenson et al. (1994) showed that increased opacities in Hyades stellar models could produce agreement with the observed Li depletions from standard pre-main-sequence (PMS) burning alone. Using  $[\text{Fe}/\text{H}] = 0.12 \pm 0.03$  from Cayrel, Cayrel de Strobel, & Campbell (1985) and scaled solar mixtures for the other elements, they were not able to reproduce the  $T_{\text{eff}}$ -Li trend observed in cool stars of the Hyades. Because of the lack of knowledge concerning stellar abundances of elements other than Fe and Li, solar mixtures have traditionally been assumed in this way, despite the possibility of nonsolar abundances. However, assuming nonsolar mixtures, specifically, an enhanced abundance of oxygen, Swenson et al. found that the increased opacity resulted in models that fit the observed Hyades data well. If true, increased opacities and the resulting PMS burning might eliminate the need for main-sequence (MS) Li depletion mechanisms in this case (though elevated abundances of the Hyades' short-period, tidally locked binaries seem a striking refutation of this; Thorburn et al. 1993). A salient issue, then, is observational guidance in setting model opacities. Unfortunately, substantial information on observed open cluster (or field star) abundances beyond Fe and Li is lacking. In the case of the Hyades, the closest and most well studied cluster, limited data exist suggesting subsolar, solar, or supersolar  $[\text{O}/\text{Fe}]$  ratios; accounting for study-to-study differences is surprisingly nontrivial (King & Hiltgen 1996). Regardless, Chaboyer et al. (1995) and Piau & Turck-Chièze (2002) confirm that metallicity and chemical composition are important to the modeling of Li abundance depletions; that observed intracluster Li dispersions might be related to star-to-star scatter of the elements remains possible. Obviously, knowledge of chemical compositions and any cluster scatter is needed for a more complete understanding of observed Li abundances.

Elemental abundances also play an important role in distances to clusters inferred from MS fitting. This procedure utilizes stars' positions in the H-R diagram, which are specified by their mass, chemical composition (not just  $[\text{Fe}/\text{H}]$  alone), and age. By comparing the MS of a star cluster with an empirical MS for which the distance and composition are known, the distance to the cluster can be deduced. The distances as determined by *Hipparcos* parallax data are found to be in good agreement with MS fitting for most of the clusters observed by *Hipparcos*; there are exceptions, however, with much attention given to the Pleiades. The Pleiades' distance modulus as determined by MS fitting is found to be 5.60 mag (VandenBerg & Bridges 1984; Pinsonneault et al. 1998), while the *Hipparcos*-based modulus is  $5.36 \pm 0.06$  mag (Robichon et al. 1999). Solar abundances, mixtures, or

both are often adopted for clusters, which could result in incorrect positions in the H-R diagram (by as much as 0.20 mag for  $\Delta[\text{Fe}/\text{H}] = 0.15$  dex) and, thus, incorrect MS-fitting-based distance determinations. While Pinsonneault et al. (1998) suggest that this is not the cause of the disagreement in the case of the Pleiades, for which limited abundance work has been carried out (e.g., Boesgaard 1989; Boesgaard & Friel 1990; King 1993; King et al. 2000), they remind us that the abundances of Si and Mg, which contribute to atmospheric opacities, are not well known for the Pleiades. Again, proper elemental abundances for clusters are required in order to help build confidence in the distances derived from MS fitting on a cluster-to-cluster basis. Cognately, these abundances are necessary ingredients for reliable age determinations for open clusters, which are valuable chronometers in the Galactic disk.

Despite the importance of having accurate metal abundances for open clusters, there are limited data other than for Fe and Li; exceptions are detailed abundances for 12 Hyades stars (Cayrel et al. 1985), 16 Pleiades stars (Wilden et al. 2002), and for a few Pleiades and NGC 2264 stars (King et al. 2000). While we plan targeted efforts in this regard, it should be noted that the future success of stellar models to match observations (and thus our understanding of stellar properties) undoubtedly lies in a combination of accurate abundances and nonstandard physics, neither seemingly being a solution to existing discrepancies alone. As such, the present study is an exploratory response to the growing need for accurate open cluster abundances. Using the spectroscopic data from Jones et al. (1997, hereafter JFSS), we have analyzed nine solar-type dwarfs in the open cluster M34, deriving abundances for Fe, Ni, Ti, Cr, Ca, Si, and Al. Our goal is to provide initial estimates of mean abundances and to place constraints on intracluster scatter.

## 2. OBSERVATIONS AND MEMBERSHIP

### 2.1. *Observational Data*

Echelle spectra of 34 stars in M34 were obtained with the HIRES spectrograph (Vogt 1992) on the 10 m Keck I Telescope with incomplete wavelength coverage from  $\sim 6300$  to  $\sim 8700$  Å. The data were originally taken by JFSS in 1994 in order to investigate the Li abundances of M34 stars. The spectra presented herein have a resolution of  $R \sim 45,000$  with a typical signal-to-noise ratio of  $\sim 70$ . The data are more fully described in JFSS.

Of the 34 stars observed, nine G and K dwarfs were chosen for analysis. The criteria used in deciding which stars to examine were low rotational velocities and high membership probabilities, data for which were taken from JFSS. The significance of choosing stars with relatively low rotational velocities is the reduction of blending of spectral lines, which increases with increasing rotational velocity, and the minimization of photon-noise contributions to the line-strength measurement uncertainties. All the stars have rotational velocities  $v \sin i \leq 11$  km s $^{-1}$ . We also chose stars such that our sample covered a range of effective temperatures, allowing us to consider any abundance spreads in the cool stars with respect to their observed Li abundances. Star identification numbers taken from Jones & Prosser (1996, hereafter JP) are listed in column (1) of Table 1, rotational velocities in column (5), and proper-motion-based membership probabilities in column (6).

TABLE 1  
 STELLAR DATA

Star (1)	$(B-V)_0$ (mag) (2)	$T_{\text{eff}}$ (K) (3)	$\xi$ ( $\text{km s}^{-1}$ ) (4)	$v \sin i$ ( $\text{km s}^{-1}$ ) (5)	Memb. Prob. (%) (6)
JP 133 .....	0.62	5810	1.05	11.0	96
JP 199 .....	0.80	5173	0.42	9.5	85
JP 208 .....	0.66	5658	0.90	5.0	98
JP 296 .....	0.69	5548	0.78	5.0	91
JP 298 .....	0.92	4814	0.09	8.9	71
JP 366 .....	0.65	5695	0.94	7.0	94
JP 415 .....	0.72	5442	0.69	5.0	93
JP 489 .....	0.89	4899	0.16	7.8	67
JP 515 .....	0.57	6007	1.26	9.8	98

## 2.2. Membership

Membership was carefully scrutinized when considering the stars to be analyzed. Proper-motion-based membership probabilities were calculated by both Ianna & Schlemmer (1993) and JP. Membership agreement was found for most stars; however, two exceptions are considered in the present study—JP 296 and JP 515. Ianna & Schlemmer found membership probabilities of 20% for JP 296 and 38% for JP 515, while JP found 91% and 98%, respectively. A cluster color-magnitude diagram is shown in Figure 1, photometric data for which were taken from JP and JFSS. The JFSS  $(B-V)_0$  values were derived by averaging the observed  $B-V$  and the observed  $(V-I)_K$ , both from JP, and transforming these to  $B-V$ . The averaged value was then corrected for reddening by  $E(B-V) = 0.07$  mag. The  $(B-V)_0$  colors are listed in column (2) of Table 1. The placement of JP 296 and JP 515 on the cluster color-magnitude diagram, as with all the stars considered here, is close to the cluster MS, suggesting

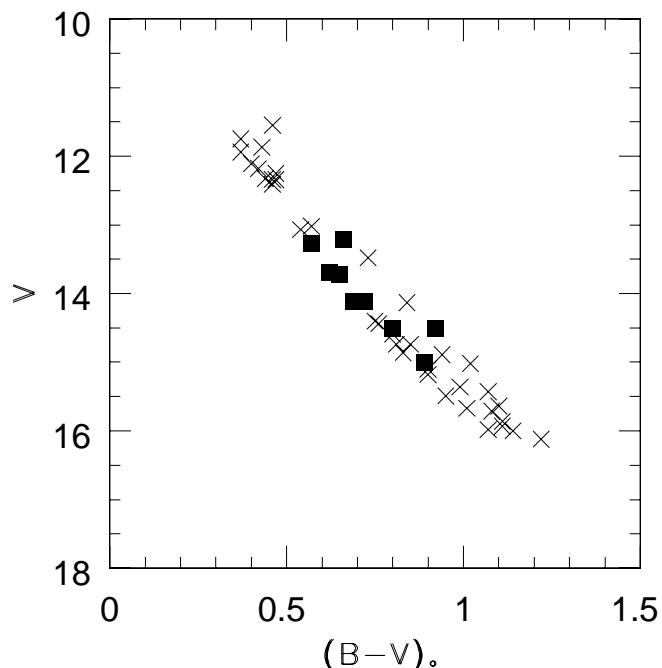


FIG. 1.—M34 color-magnitude diagram. A reddening of 0.07 mag has been adopted for  $(B-V)_0$  colors. Squares are the stars considered in the present study, and crosses are the remaining stars found in JFSS.

membership. The JFSS radial velocities confirm membership of all the stars considered here except JP 296, for which only one observation had been made. Despite its disparate radial velocity, the high membership probability found by JP and its placement on the color-magnitude diagram led JFSS to conclude that JP 296 is a member of the cluster but may be a single-lined spectroscopic binary (SB1). Both the  $B-V$  and the  $V-I$  color-magnitude diagrams based on M34 photometry from the WIYN Open Cluster Study also suggest membership for JP 296 (C. Deliyannis 2002, private communication). However, they also find that its radial velocity is outside that of the cluster, adding support that it is an SB1. We have adopted JP 296 as a member of the cluster.

## 3. ANALYSIS

### 3.1. Spectral Lines

Spectral line selection was aided by the solar line list of Thévenin (1990), except for the two Mg lines measured, which were chosen from King et al. (2000). Lines in the Thévenin list classified as “case b” (those with errors  $\sigma > 0.05$  in the  $\log gf$  values) were not considered, as a consequence of possible blending. Because of the moderate typical signal-to-noise ratio, each of the remaining “case a” lines was scrutinized and compared with solar lines found in the Kurucz et al. (1984) solar atlas. Any line that was thought to be blended or otherwise unmeasurable was discarded. Because of the wide spectral coverage, we were left with 69 to 118 Fe I lines for all the stars except JP 298 and JP 489, which are the two coolest stars and are subject to increased blending effects. For these we relied on a selection of the 26 and 29 cleanest Fe I lines, respectively. Sample spectra are given in Figure 2.

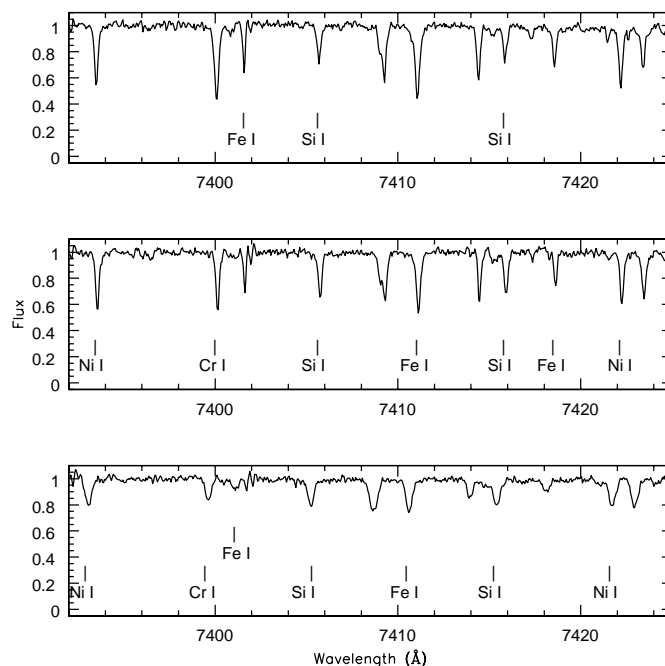


FIG. 2.—Keck HIRES spectra of selected M34 stars. *Top*, JP 298; *middle*, JP 415; *bottom*, JP 515. The labeled lines in each panel are those measured for the respective star.

### 3.2. Equivalent Widths and Stellar Parameters

Equivalent widths of our stellar and solar lines were measured using the one-dimensional spectrum analysis package SPECTRE (Fitzpatrick & Sneden 1987), utilizing Gaussian curves for integrations. The LTE stellar line analysis program MOOG (Sneden 1973) was then used to derive abundances, using stellar atmospheres interpolated from the grids of R. Kurucz (1992, private communication). The equivalent widths and abundances are listed in Table 2. The solar abundances were obtained in a consistent fashion, using measured equivalent widths, the same  $\log gf$  values, and a Kurucz solar model atmosphere. Initial color-based values of  $T_{\text{eff}}$  for the M34 members were taken from JFSS. Surface gravities were calculated using the polynomial fitted to zero-age main-sequence (ZAMS) models found in Gray (1992),

$$\begin{aligned} \log g = & 4.38 - 0.1371(B-V) - 0.8141(B-V)^2 \\ & + 5.5555(B-V)^3 - 6.6815(B-V)^4 \\ & + 2.3615(B-V)^5, \end{aligned}$$

which is believed to vary insignificantly for  $B-V \geq 0.5$  from a polynomial approximation fitted to an observed MS of binary star calibrations (see Gray 1992 for references). The reddening-corrected  $(B-V)_0$  colors from JFSS were used to calculate the  $\log g$  values. Random uncertainties in  $\log g$  due to those color indexes are below 0.01 dex. The polynomial relation itself is believed to be accurate to within 0.10 dex, which has been conservatively adopted as the  $1\sigma$  level uncertainty in  $\log g$ .

Initial microturbulent velocities were calculated using the relation found in Edvardsson et al. (1993):

$$\begin{aligned} \xi = & 1.25 + (8 \times 10^{-4})(T_{\text{eff}} - 6000) \\ & - 1.3(\log g - 4.5) \text{ km s}^{-1}. \end{aligned}$$

This relation was reported to be applicable for stars within the parameter ranges  $5500 \text{ K} < T_{\text{eff}} < 6800 \text{ K}$ ,

$3.8 < \log g < 4.5$ , and  $-1.1 < [X/H] < 0.3$ . While some initial stellar parameters lay outside these ranges, the calculated  $\xi$ -values were used only as initial guesses. Initial values for  $T_{\text{eff}}$  and  $\xi$  are listed in columns (3) and (4) of Table 1.

Final effective temperatures were derived spectroscopically by altering the temperature in the model atmospheres and investigating the correlations between the resultant line-by-line Fe I relative abundances (i.e., normalized to the Sun) and the excitation potentials ( $\chi$ ). The final temperature for a given star was achieved when no correlation remained, thus obtaining Fe I excitation balance. Likewise, eliminating correlations between the Fe I relative abundances and reduced equivalent widths [ $\log(\text{EW}/\lambda)$ ] provided the final  $\xi$ -values. We also plot the line-by-line  $[\text{Fe}/\text{H}]$  values against wavelength, showing no statistically significant dependence of derived abundance on wavelength. Figure 3 shows the line-by-line Fe abundances for JP 208 plotted against  $\chi$ ,  $\log(\text{EW}/\lambda)$ , and wavelength. Uncertainties in these parameters were calculated by considering the correlations in the above quantities as each parameter was varied individually. Final uncertainties are those that resulted a  $1\sigma$  deviation in the correlation coefficients of  $[\text{Fe}/\text{H}]$  and  $\chi$  for  $T_{\text{eff}}$ , and  $[\text{Fe}/\text{H}]$  and  $\log(\text{EW}/\lambda)$  for  $\xi$ . Final temperatures and microturbulent velocities are listed in columns (2) and (4) of Table 3, with their uncertainties in columns (3) and (5). The  $\log g$  values and the adopted uncertainty are listed in columns (6) and (7).

We note that while many other studies use the same approach in determining spectroscopic  $T_{\text{eff}}$ - and  $\xi$ -values, in many cases the solutions may be degenerate. This can happen when a particular sample of lines demonstrates an ab initio correlation between line strength and lower excitation potential. Happily, no such significant correlation exists in our particular selection of Fe I lines.

## 4. RESULTS

Final relative abundances,  $[X/H]$  and  $[X/\text{Fe}]$ , were obtained by subtracting line by line the solar abundances

TABLE 2  
EQUIVALENT WIDTH MEASURES

ION	$\lambda_{\text{meas}}$ (Å)	$\chi$ (eV)	$\log gf$	$\text{EW}_{\odot}$	$\log N_{\odot}$	JP 133		JP 199		JP 208		JP 296	
						EW	$\log N$						
Fe I.....	6311.50	2.83	-3.21	28.6	7.55	...	...	...	...	...	...	...	...
	6315.81	4.07	-1.76	38.5	7.52	...	...	56.0	7.55	52.6	7.63	42.5	7.43
	6322.69	2.59	-2.40	74.7	7.43	100.5	7.52	115.7	7.55	95.1	7.43	114.1	7.81
	6330.85	4.73	-1.32	33.3	7.60	43.0	7.68	53.8	7.74	40.2	7.62	39.4	7.58
	6335.34	2.20	-2.20	102.0	7.36	118.6	7.19	162.0	7.49	119.8	7.20	122.2	7.33

ION	$\lambda_{\text{meas}}$ (Å)	JP 298		JP 366		JP 415		JP 489		JP 515	
		EW	$\log N$								
Fe I.....	6311.50	59.1	7.57	...	...	39.6	7.52	51.3	7.57	...	...
	6315.81	41.9	7.26	45.6	7.58	53.3	7.63	44.8	7.39	...	...
	6322.69	...	...	87.0	7.44	98.4	7.59	...	...	...	...
	6330.85	38.2	7.48	34.5	7.57	40.4	7.59	47.8	7.69	31.9	7.69
	6335.34	...	...	123.2	7.42	125.1	7.33	...	...	99.2	7.26

NOTE.—Equivalent widths are given in milliangstroms. Table 2 is presented in its entirety in the electronic edition of the *Astronomical Journal*. A portion is shown here for guidance regarding its form and content.

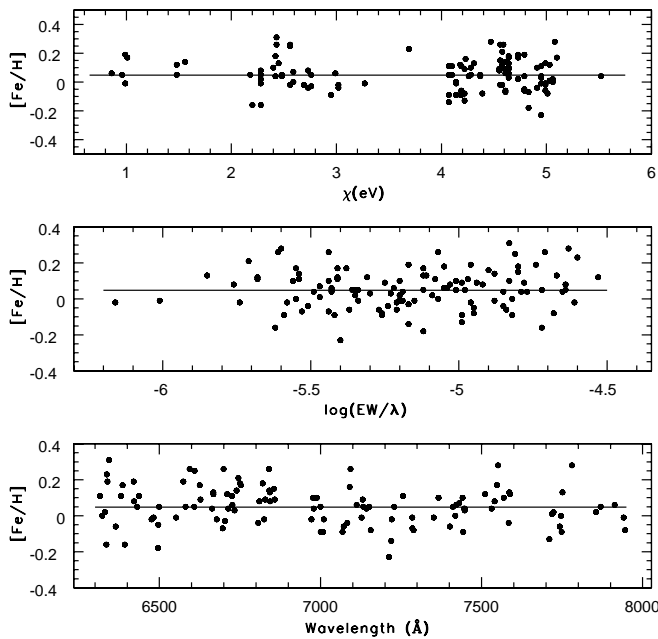


FIG. 3.—Line-by-line Fe relative abundance correlation relations for JP 208, as a function of excitation potential (*top*), reduced equivalent width (*middle*), and wavelength (*bottom*). The line drawn in all three panels represents the mean Fe abundance for JP 208.

from the stellar abundances. Mean abundance ratios for the nine-star sample are given in Table 4, along with the number of lines measured for each species and the internal ( $\sigma_{\text{int}}$ ) and total ( $\sigma_{\text{tot}}$ ) mean uncertainties. The internal errors are based solely on the line-to-line scatter about the star's mean abundance. The total errors were derived from these internal errors and errors in  $T_{\text{eff}}$ ,  $\xi$ , and  $\log g$ . Sensitivities to these parameters were calculated by varying each parameter singly and creating additional models, one with  $\Delta T_{\text{eff}} = 150$  K, one with  $\Delta \xi = 0.30$  km s $^{-1}$ , and one with  $\Delta \log g = 0.25$  dex, for each star. The abundances resulting from these individual models were compared with the originally derived abundances to obtain the sensitivities. The low temperatures of JP 298 and JP 489 make their abundances more susceptible to ionization-state changes that occur for some of the elements near these lower effective temperatures. Accordingly, sensitivities for these two stars were calculated for both positive and negative changes in temperature (as

TABLE 3  
FINAL STELLAR PARAMETERS AND UNCERTAINTIES

Star (1)	$T_{\text{eff}}$ (K) (2)	$\sigma_{T_{\text{eff}}}$ (K) (3)	$\xi$ (km s $^{-1}$ ) (4)	$\sigma_{\xi}$ (km s $^{-1}$ ) (5)	$\log g$ (cgs) (6)	$\sigma_{\log g}$ (cgs) (7)
JP 133 .....	5710	$\pm 58$	1.88	$\pm 0.10$	4.54	$\pm 0.10$
JP 199 .....	5385	$\pm 40$	1.65	$\pm 0.11$	4.63	$\pm 0.10$
JP 208 .....	5675	$\pm 35$	1.80	$\pm 0.08$	4.56	$\pm 0.10$
JP 296 .....	5460	$\pm 48$	1.09	$\pm 0.11$	4.58	$\pm 0.10$
JP 298 .....	4750	$\pm 25$	1.55	$\pm 0.14$	4.66	$\pm 0.10$
JP 366 .....	5760	$\pm 38$	1.63	$\pm 0.07$	4.55	$\pm 0.10$
JP 415 .....	5290	$\pm 45$	0.67	$\pm 0.18$	4.59	$\pm 0.10$
JP 489 .....	4750	$\pm 25$	0.80	$\pm 0.12$	4.66	$\pm 0.10$
JP 515 .....	6130	$\pm 65$	2.07	$\pm 0.10$	4.50	$\pm 0.10$
Sun .....	5770		1.10		4.44	

well as microturbulent velocity and surface gravity). Typical sensitivities are given in Table 5.

## 5. DISCUSSION

### 5.1. Iron in M34

The mean iron abundance for the nine stars is  $[\text{Fe}/\text{H}] = +0.02 \pm 0.02$  (uncertainty in the mean). The standard deviation about this mean is  $\pm 0.06$  dex. Given that the average individual total uncertainty in  $[\text{Fe}/\text{H}]$  is  $\pm 0.04$  dex, this limits any real star-to-star scatter to  $\leq 0.05$  dex. While the full range in  $[\text{Fe}/\text{H}]$  is a modest 0.14 dex, the two coolest stars demonstrate relative underabundances (Fig. 4). Although their deviations are not significant when considered individually, collectively they result in a linear correlation in the  $[\text{Fe}/\text{H}]-T_{\text{eff}}$  plane significant at greater than the 99% confidence level. Similar behavior is seen for Ti, Ca, Si, Al, and (perhaps marginally so) Mg, with statistically significant correlation coefficients found for these elements. Excluding JP 298 and JP 489, the two coolest stars in the sample and in general the most anomalous with regard to abundances, eliminates any significant correlation in the  $[\text{X}/\text{H}]-T_{\text{eff}}$  planes for all the elements except Mg, where a marginal correlation remains. *If real*, there are a number of effects that could be causing the observed relations, most notably non-LTE (NLTE) effects resulting in overionization, overexcitation, or both. Systematic errors associated with the atmospheric models and derivation of the stellar parameters could also produce such trends. Each of these possibilities will be discussed in the following sections, starting with the atmospheric models and stellar parameters.

#### 5.1.1. Models, Stellar Parameters, and Measurements

The present study is the first to undertake the spectroscopic measurements of chemical abundances of M34 cluster stars for elements other than Li. We are thus using the model atmospheres in a manner rarely done—applying them to presumed chemically homogeneous stars having a range of temperatures. This opens the possibility of exposing shortcomings in the model atmosphere grids. Could there be  $T_{\text{eff}}$ -dependent deficiencies in the grids that would produce modest abundance anomalies in our cooler stars? If the models are to be suspected in creating any trends, it would be expected that the trends would be consistent. “Consistent” is to be taken to mean that similar parameters should produce similar results. This is not the case in the  $[\text{Fe}/\text{H}]-T_{\text{eff}}$  relation in Figure 4. The  $[\text{Fe}/\text{H}]$  ratios for the cool stars ( $T_{\text{eff}} < 5500$  K) are all below solar except for JP 199, which is cooler than the iron-deficient JP 296. Thus, there may not be a consistent bias in the model atmospheres that necessarily results in low Fe abundances for the coolest stars (similar conclusions apply to  $\xi$  and  $\log g$ ). We cannot, however, make strong assertions based on one star. An expanding of cluster sample sizes is needed to explore this issue further.

It should also be mentioned that Kurucz models have been used extensively in additional studies that derived Fe abundances of various open clusters. Examples of these are Boesgaard (1989), Boesgaard & Friel (1990), and Barrado y Navascués, Deliyannis, & Stauffer (2001). To our knowledge, there is no report in any cluster study, including those listed, of a correlation of  $[\text{Fe}/\text{H}]$  with  $T_{\text{eff}}$ . However, none of these studies included stars as cool ( $< 5300$  K) as those in

TABLE 4  
FINAL ABUNDANCES AND UNCERTAINTIES

Star	[Fe/H]	[Ni/H]	[Ni/Fe]	[Ti/H]	[Ti/Fe]	[Cr/H]	[Cr/Fe]	[Ca/H]	[Ca/Fe]	[Si/H]	[Si/Fe]	[Al/H]	[Al/Fe]	[Mg/H]	[Mg/Fe]
JP133	0.07	-0.06	-0.13	-0.10	-0.17	0.18	0.11	0.10	0.02	0.05	-0.02	...	...	0.01	-0.06
Lines	71	16		3		3		5		7		...	...	2	
$\sigma_{\text{int}}$	0.02	0.04	0.04	0.08	0.08	0.05	0.05	0.08	0.08	0.07	0.07	...	...	0.11	0.11
$\sigma_{\text{tot}}$	0.05	0.06	0.05	0.10	0.08	0.07	0.05	0.09	0.08	0.07	0.08	...	...	0.11	0.12
JP199	0.08	-0.03	-0.12	0.08	0.00	0.06	-0.02	0.15	0.06	0.04	-0.04	0.03	-0.05	-0.01	-0.09
Lines	111	21		6		6		5		7		3		2	
$\sigma_{\text{int}}$	0.01	0.02	0.02	0.02	0.02	0.04	0.04	0.04	0.04	0.05	0.05	0.03	0.03	0.01	0.01
$\sigma_{\text{tot}}$	0.03	0.03	0.02	0.05	0.03	0.06	0.04	0.07	0.05	0.05	0.06	0.04	0.03	0.02	0.03
JP208	0.05	-0.08	-0.13	0.02	-0.03	0.06	0.02	0.10	0.05	0.01	-0.04	-0.09	-0.14	-0.08	-0.12
Lines	118	22		7		6		6		12		3		2	
$\sigma_{\text{int}}$	0.01	0.03	0.03	0.07	0.07	0.08	0.08	0.03	0.03	0.03	0.03	0.11	0.11	0.08	0.08
$\sigma_{\text{tot}}$	0.02	0.04	0.03	0.08	0.07	0.09	0.08	0.05	0.04	0.03	0.04	0.11	0.11	0.08	0.08
JP296	-0.02	0.05	0.06	-0.13	-0.11	-0.11	-0.10	-0.04	-0.03	0.14	0.15	-0.02	0.01	-0.19	-0.17
Lines	113	25		7		7		6		10		3		2	
$\sigma_{\text{int}}$	0.02	0.03	0.04	0.06	0.06	0.03	0.04	0.05	0.05	0.03	0.04	0.09	0.09	0.01	0.02
$\sigma_{\text{tot}}$	0.04	0.04	0.04	0.08	0.07	0.04	0.04	0.07	0.06	0.03	0.05	0.09	0.10	0.03	0.04
JP298	-0.06	-0.07	-0.02	-0.19	-0.13	-0.16	-0.10	-0.14	-0.08	0.10	0.15	-0.14	-0.08	-0.16	-0.10
Lines	26	13		7		2		1		8		3		2	
$\sigma_{\text{int}}$	0.02	0.02	0.03	0.03	0.04	0.06	0.06	...	0.02	0.03	0.04	0.03	0.04	0.08	0.08
$\sigma_{\text{tot}}$	0.03	0.03	0.03	0.05	0.05	0.09	0.09	0.02	0.04	0.04	0.05	0.03	0.05	0.08	0.10
JP366	0.06	-0.03	-0.09	0.03	-0.03	0.10	0.03	0.05	-0.01	0.00	-0.07	0.09	0.03	-0.06	-0.12
Lines	106	20		5		5		6		11		2		2	
$\sigma_{\text{int}}$	0.01	0.02	0.02	0.06	0.06	0.04	0.04	0.04	0.04	0.02	0.02	0.11	0.11	0.04	0.04
$\sigma_{\text{tot}}$	0.03	0.04	0.02	0.07	0.06	0.05	0.04	0.05	0.04	0.02	0.03	0.11	0.11	0.05	0.04
JP415	-0.05	-0.05	0.00	-0.17	-0.12	0.04	0.08	-0.03	0.01	0.01	0.05	-0.12	-0.07	-0.37	-0.32
Lines	69	15		4		6		6		6		1		2	
$\sigma_{\text{int}}$	0.02	0.03	0.04	0.05	0.05	0.04	0.04	0.04	0.04	0.06	0.06	...	0.02	0.01	0.02
$\sigma_{\text{tot}}$	0.04	0.05	0.04	0.07	0.06	0.07	0.05	0.07	0.05	0.06	0.07	0.02	0.02	0.03	0.05
JP489	-0.05	-0.06	-0.01	-0.33	-0.28	-0.22	-0.17	-0.34	-0.29	0.15	0.20	-0.27	-0.22	-0.25	-0.20
Lines	29	14		6		3		2		10		3		2	
$\sigma_{\text{int}}$	0.02	0.02	0.03	0.05	0.05	0.01	0.02	0.01	0.02	0.04	0.04	0.03	0.04	0.14	0.14
$\sigma_{\text{tot}}$	0.03	0.03	0.03	0.06	0.06	0.03	0.04	0.04	0.05	0.05	0.05	0.03	0.04	0.14	0.15
JP515	0.08	-0.08	-0.16	...	...	-0.13	-0.21	0.09	0.01	-0.02	-0.10	0.03	-0.05	0.00	-0.08
Lines	75	17		...	...	2		3		7		2		2	
$\sigma_{\text{int}}$	0.02	0.04	0.04	...	...	0.06	0.06	0.06	0.06	0.03	0.04	0.03	0.04	0.08	0.08
$\sigma_{\text{tot}}$	0.05	0.06	0.05	...	...	0.07	0.06	0.08	0.06	0.04	0.04	0.04	0.04	0.09	0.09
Mean	0.02	-0.04	-0.07	-0.10	-0.11	-0.02	-0.04	-0.01	-0.03	0.05	0.03	-0.06	-0.08	-0.12	-0.14
$\sigma_{\text{mean}}$	0.02	0.01	0.03	0.05	0.03	0.05	0.03	0.05	0.04	0.02	0.04	0.04	0.03	0.05	0.03

TABLE 5  
PARAMETER SENSITIVITIES

Ratio	$\Delta T_{\text{eff}}$	$\Delta \xi$	$\Delta \log g$	Ratio	$\Delta T_{\text{eff}}$	$\Delta \xi$	$\Delta \log g$	Ratio	$\Delta T_{\text{eff}}$	$\Delta \xi$	$\Delta \log g$
JP 296:			JP 298:			JP 515:					
[Fe I/H].....	+0.09	-0.05	-0.01	[Fe I/H].....	-0.01	-0.03	+0.03	[Fe I/H].....	+0.01	-0.04	-0.03
[Fe II/H].....	-0.09	-0.07	+0.11	[Fe II/H].....	+0.02	+0.04	-0.04	[Fe II/H].....	-0.03	-0.05	+0.11
[Ni/H].....	+0.06	-0.05	+0.01	[Ni/H].....	+0.23	+0.04	-0.16	[Ni/H].....	+0.10	-0.04	-0.01
[Ti/H].....	+0.16	-0.02	-0.01	[Ni/H].....	-0.02	-0.03	+0.05	[Ti/H].....	...	...	...
[Cr/H].....	+0.11	-0.04	-0.03	[Ti/H].....	+0.03	+0.03	-0.06	[Cr/H].....	+0.10	-0.03	-0.02
[Ca/H].....	+0.13	-0.05	-0.06	[Ti/H].....	+0.18	-0.05	0.00	[Ca/H].....	+0.10	-0.03	-0.02
[Si/H].....	-0.01	-0.01	+0.01	[Ti/H].....	-0.18	+0.06	0.00	[Si/H].....	+0.10	-0.05	-0.04
[Al/H].....	+0.07	-0.01	-0.02	[Cr/H].....	+0.07	-0.03	-0.16	[Al/H].....	+0.07	-0.01	-0.01
[Mg/H].....	+0.06	+0.01	-0.05	[Cr/H].....	-0.06	+0.02	0.00	[Mg/H].....	+0.05	-0.02	-0.04
				[Ca/H].....	+0.13	-0.02	-0.02				
				[Ca/H].....	-0.14	+0.02	+0.01				
				[Si/H].....	-0.01	-0.01	+0.04				
				[Si/H].....	+0.12	+0.01	-0.05				
				[Al/H].....	+0.07	-0.01	-0.01				
				[Al/H].....	-0.07	+0.02	+0.02				
				[Mg/H].....	-0.01	+0.01	-0.01				
				[Mg/H].....	+0.04	-0.05	+0.02				

NOTE.—Listed are sensitivities calculated for changes of +150 K, +0.30 km s<sup>-1</sup>, and +0.25 dex in effective temperature, microturbulent velocity, and surface gravity, respectively (JP 296, JP 515), and ±150 K, ±0.30 km s<sup>-1</sup>, and ±0.25 dex (JP 298).

our sample. Wilden et al. (2002) derived abundances of 11 elements for 16 Pleiades dwarfs, including stars with  $T_{\text{eff}} \leq 5300$  K, using the Spectroscopy Made Easy software package and utilizing Kurucz model atmospheres. No  $T_{\text{eff}}$ -

dependent abundance effects were noted; however, it appears in Table 5 therein that their Cr, Ti, and Sc abundances are relatively lower in the cool stars and their Si is relatively higher in the cool stars, similar to the behaviors

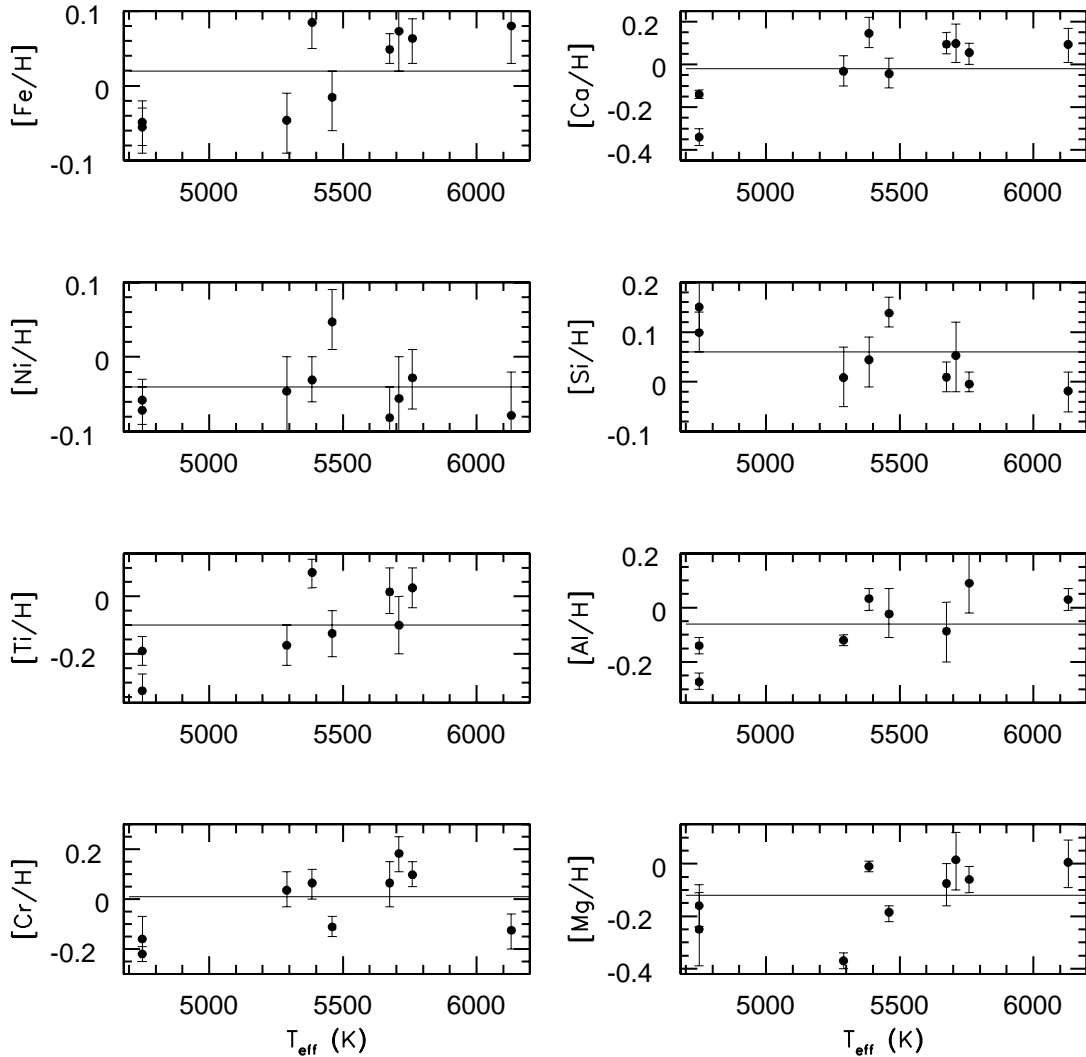


FIG. 4.—[X/H] as a function of  $T_{\text{eff}}$ . The solid lines represent the cluster mean based on all nine stars.

seen here. Plotting these abundances against temperature results in statistically significant linear correlation coefficients, verifying the relations.

Generally, abundances derived from neutral species are not sensitive to surface gravity, and it plays a minor role in the stellar models. The use of the polynomial fitted to the ZAMS isochrones is appropriate for M34, which has an estimated age of 250 Myr (JP). Another method of calculating  $\log g$  was considered, namely, ionization balance. However, ionization balance—requiring that equivalent abundances be derived from, for example, the Fe I and Fe II lines—is subject to overionization effects that might be present (especially in cool stars), resulting in surface gravities that are unbelievably low. Gratton, Carretta, & Castelli (1996) found such results in their analysis of metal-poor field stars using the 1992 Kurucz models. They reported that their data suggested the Kurucz models were not suitable for stars with  $T_{\text{eff}} < 4400$  K but further commented that deviations from LTE needed to be investigated.

With respect to the initial metallicity of M34, prior knowledge was limited. The metallicity has been determined by only one previous study, that of Canterna, Perry, & Crawford (1979). They found the mean metallicity-sensitive Strömgen index to be  $\delta m_1 = 0.01$ , the same as the Pleiades, which was taken to be similar to the solar value. Thus, all the model atmospheres for the present M34 stars were created with the metallicity set to zero. The deviations from this assumption are less than  $\pm 0.1$  dex for all the stars, and thus the effects associated with deviations from zero metallicity are negligible.

In order to investigate their effect on the  $[X/H]-T_{\text{eff}}$  relations, the initial photometric  $T_{\text{eff}}$  and  $\xi$  [along with the  $(B-V)_0$ -determined  $\log g$ ] were used to generate additional model atmospheres. The resulting abundances followed the same behavior as those derived from the final parameters. It should also be noted that the differences between our final temperatures and those of JFSS show no trend with temperature. Adopting  $\xi = 0$  for each star did not eliminate the relations either. The parameter sensitivities (Table 5) can be used to determine whether any modification of the parameters can eliminate the  $[X/H]-T_{\text{eff}}$  relations. In general, the sensitivities to  $T_{\text{eff}}$  are such that changing the individual temperatures could not result in the simultaneous flattening of the  $[X/H]-T_{\text{eff}}$  correlations for each element. Particularly for Fe and Si, the sensitivities are dissimilar in magnitude and often in the same sense; that is, reducing the temperature for JP 515 lowers the  $[\text{Fe}/\text{H}]$  ratio, which could contrib-

ute to the leveling of the  $[\text{Fe}/\text{H}]-T_{\text{eff}}$  relation, and at the same time lowers the  $[\text{Si}/\text{H}]$  ratio, increasing the dispersion in the Si abundance between JP 515 and the cooler stars. The effects of altering  $\xi$  and  $\log g$  are similar in that the  $[X/H]-T_{\text{eff}}$  relations cannot be removed. We are confident, then, that the parameters adopted are not the cause of any anomalous behavior seen in the abundance ratios.

We also exclude several other sources of the modest but consistent abundance deviations for our two coolest M34 dwarfs. Relative line-strength measurement errors induced by scattered light or continuum location do not provide a self-consistent explanation for both the Si overabundances in the cool stars and the underabundances of the other elements. Moreover, they cannot explain the difference in the Fe I-based and Fe II-based abundances. We also note that while we used a more restricted selection of Fe I lines for the two coolest dwarfs to avoid possible blending effects, the odd cool-star abundance patterns persist when using the same set of lines as for the warmer stars.

### 5.1.2. NLTE Effects: Overionization and Increased Excitation

The possible NLTE effects seen in the  $[X/H]-T_{\text{eff}}$  relations motivated the analysis of the Fe II lines to investigate ionization balance; the abundance results are given in Table 6. The first column lists the wavelengths of the Fe II lines that were measured (not all lines were measurable in all stars), the second gives the solar abundance ( $\log N_{\odot}$ ) for each line, and the remaining columns are the  $[\text{Fe II}/\text{H}]$  for each star. Plotting the abundance difference derived from Fe II and Fe I against temperature shows a dramatic overionization of Fe for JP 296, 298, 415, and 489 (Fig. 5). Unfortunately, no clean ionic lines of suitable strength were available for the other elements, which could have been used to check for overionization in those cases.

Feltzing & Gustafsson (1998) studied metal-rich G and K *field* dwarfs and found overionization in the five K dwarfs ( $4510 \text{ K} \leq T_{\text{eff}} \leq 4833 \text{ K}$ ) of their sample. They used photometric temperatures in their derivation of elemental abundances; excitation equilibrium with Fe I resulted for all stars except the K dwarfs. Furthermore, they experienced difficulty in obtaining definite  $\xi$ -values for the K dwarfs using the methods that enforced zero correlation between Fe I equivalent widths and  $\xi$  for the other stars. As a result, the same  $\xi = 1.0 \text{ km s}^{-1}$  was adopted for the K dwarfs. A result of their abundance analysis was the appearance of overionization of Fe and four other elements (Sc, V, Cr, and Y) in their five cool K dwarfs. Although they acknowledged that

TABLE 6  
LINE-BY-LINE AND MEAN  $[\text{Fe II}/\text{H}]$  ABUNDANCES

$\lambda$ (Å)	$\log N_{\odot}$	JP 133	JP 199	JP 208	JP 296	JP 298	JP 366	JP 415	JP 489	JP 515
6416.93 .....	7.69	0.01	0.12	-0.14	0.43	0.73	-0.01	0.52	0.51	-0.04
6432.68 .....	7.72	-0.03	-0.14	-0.06	0.44	0.44	-0.03	0.36	0.52	0.00
6456.39 .....	7.55	0.08	0.04	-0.04	0.40	0.52	0.15	0.45	0.68	-0.09
7222.40 .....	7.55	...	0.27	0.27	...	...	0.10	...	...	...
7224.46 .....	7.58	0.10	...	...	0.42	...	0.13	0.22	...	...
7449.34 .....	7.69	...	0.12	0.35	...	...	...	0.32	...	...
7515.84 .....	7.56	...	...	0.28	...	...	...	...	...	...
Mean.....	7.62	0.04	0.08	0.11	0.42	0.56	0.07	0.37	0.57	-0.04
$\sigma_{\text{int}}$ .....	0.03	0.03	0.07	0.10	0.01	0.11	0.04	0.06	0.07	0.03
$\sigma_{\text{tot}}$ .....		0.06	0.09	0.11	0.06	0.13	0.06	0.09	0.10	0.06

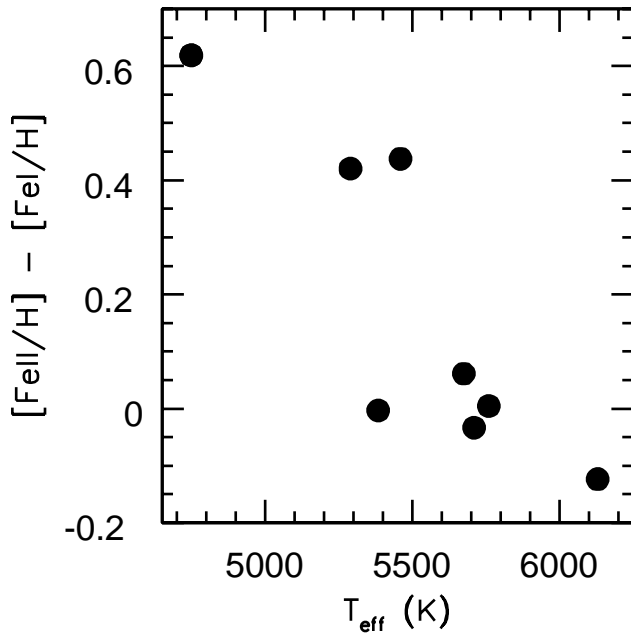


FIG. 5.—Difference in Fe abundance from Fe II and Fe I vs.  $T_{\text{eff}}$ . Note that JP 298 and JP 489 (4750 K) both have the same Fe II – Fe I difference of 0.62 dex.

ill-adopted effective temperatures could partially explain the observed overionization, their final conclusion was that NLTE effects were the cause and thus affected the derived abundances for all the elements for these stars. Interestingly, their  $[\text{Fe}/\text{H}]$  ratios derived from the Fe I lines showed no correlation with  $T_{\text{eff}}$ , which one might expect if the overionization were real, because of the systematically low Fe abundance (derived from Fe I lines) calculated by the LTE models for these cool stars. Thorén & Feltzing (2000) reanalyzed three of the five K dwarfs of Feltzing & Gustafsson (1998), deriving effective temperatures by requiring excitation balance of the Fe I lines. As a result, the overionization seen in the initial study was all but extinguished, pointing to the erroneous effective temperatures adopted by Feltzing & Gustafsson as the cause. In addition, the adoption of the new effective temperatures also brought their Fe and Cr abundances nearly into ionization balance. The present study is not subject to such temperature problems, because effective temperatures for all stars were derived by demanding Fe I excitation balance. Furthermore, we do see a modest relative underabundance of Fe in the cool stars, except JP 199, which is demonstrated in Figure 4.

Standard LTE analyses use the Boltzmann and Saha equations to calculate the populations of excited and ionized states, which are directly related to the absorption and emission coefficients. These populations are dependent on the temperature and density of the stellar atmosphere if LTE holds. Deviations from LTE that lead to inaccurately calculated populations could give rise to the effects seen in Figures 4 and 5, if the deviations result in underpopulating lower bound levels of neutral atoms. In this sense, both overionization and overexcitation are significant factors. Of all the lines measured, the Si lines as a group have higher excitation potentials ( $5.61 \text{ eV} \leq \chi \leq 6.19 \text{ eV}$ ) than all the lines of the rest of the elements. Both the Mg lines have excitation potentials above 5 eV (5.11 and 5.75 eV), with only

one in the same range as those for Si. Of the remaining elements, only Fe and Ni (which shows no trend) have lines with  $\chi > 5 \text{ eV}$ , but these lines are few in each case. Thus, an increase in excitation would depopulate the lower energy levels being measured for Fe, Ti, Cr, Ca, Al, and possibly Mg and, in a converse fashion, populate the higher levels seen in Si. We would then expect to see an enhancement in the abundance of Si for these stars and a deficiency of the other elements. Such modest effects may explain the cool-star abundances in Figure 4. Though most theoretical and observational work on NLTE effects has been limited to metal-poor, evolved, or warmer stars (making comparison with our results difficult), recent discussions of the basic framework of the NLTE problem on stellar Fe abundances can be found in, for example, Thévenin & Idiart (1999) and Gehren, Korn, & Shi (2001).

Whatever the cause, the anomalous behavior of JP 296, 298, 415, and 489 lowers the confidence in their derived abundances. We have thus excluded them from the final cluster mean abundances, which are given in Table 7. The iron abundances of the remaining stars agree very well. Furthermore, an interesting consequence of excluding the four anomalous stars is that those remaining nearly obtain Fe ionization balance. The cluster mean iron abundances derived from both states match nicely,  $0.07 \pm 0.01$  for Fe I and  $0.05 \pm 0.03$  for Fe II. The final cluster mean iron abundance adopted is that derived from Fe I (Table 7).

## 5.2. Metal Abundances

The final mean abundances are void of any statistically significant trends with respect to temperature. In addition, no scatter is seen in any element except, possibly, chromium. Chi-square tests demonstrate that Cr is the only element for which the observed scatter is approaching statistical significance, with  $\sim 97\%$  confidence that the scatter is real. JP 199, 208, and 366 have  $[\text{Cr}/\text{H}]$  ratios that agree marginally well, with values of 0.06, 0.06, and 0.10 dex, respectively. JP 133 and JP 515 have the most deviant abundances, with 0.18 and  $-0.13$  dex, but only three Cr lines were measured for JP 133 and only two for JP 515. Having more measurable Cr lines in these stars would allow the validation of these “extreme” values.

All the elements except Ni scale well with Fe within the final uncertainties, fitting nicely with the field star data of Edvardsson et al. (1993). The final mean ratios are

$$\begin{aligned} [\text{Ti}/\text{Fe}] &= -0.06 \pm 0.05, & [\text{Cr}/\text{Fe}] &= -0.01 \pm 0.06, \\ [\text{Ca}/\text{Fe}] &= 0.03 \pm 0.02, & [\text{Si}/\text{Fe}] &= -0.05 \pm 0.02, \\ [\text{Al}/\text{Fe}] &= -0.05 \pm 0.04, & [\text{Mg}/\text{Fe}] &= -0.10 \pm 0.02. \end{aligned}$$

TABLE 7  
FINAL MEAN CLUSTER ABUNDANCES

Ratio	Abundance	$\sigma_{\text{mean}}$
$[\text{Fe}/\text{H}]$ .....	0.07	0.01
$[\text{Ni}/\text{Fe}]$ .....	-0.12	0.02
$[\text{Ti}/\text{Fe}]$ .....	-0.06	0.05
$[\text{Cr}/\text{Fe}]$ .....	-0.01	0.06
$[\text{Ca}/\text{Fe}]$ .....	0.03	0.02
$[\text{Si}/\text{Fe}]$ .....	-0.05	0.02
$[\text{Al}/\text{Fe}]$ .....	-0.05	0.04
$[\text{Mg}/\text{Fe}]$ .....	-0.10	0.02

Magnesium shows a minor deviation from the Fe abundance but still fits within the Edvardsson et al. data. Nickel is somewhat more anomalous, with  $[\text{Ni}/\text{Fe}] = -0.12 \pm 0.02$ . This would place M34 stars on the extreme boundary of the Edvardsson et al. nickel distribution. King et al. (2000) found a similar result for Ni in their two Pleiades K dwarfs ( $[\text{Ni}/\text{Fe}] = -0.08 \pm 0.03$ ), and they tentatively concluded that the underabundance was real based on the similarities of Ni and Fe line strengths, excitation distribution, ionization potential, and parameter sensitivities. In addition to these factors, the low uncertainty in the final Ni abundance seen here leaves us to conclude that the underabundance in M34 is also real.

### 5.3. Lithium in M34

JFSS investigated the Li abundance of M34 stars. They found depletion and dispersion of Li abundances at a given temperature, especially for stars with  $T_{\text{eff}} \leq 5400$  K, that is intermediate to the younger Pleiades ( $\sim 80$  Myr) and the older Hyades ( $\sim 800$  Myr). Star-to-star Fe abundance scatter (more generally, intracluster variations of opacities, which are influenced by chemical composition; Swenson et al. 1994) is a mechanism that could give rise to the observed Li spread in some open clusters, especially for cool stars. As stated previously, Chaboyer et al. (1995) demonstrated that  $\Delta[\text{Fe}/\text{H}] = 0.05$  dex resulted in a change of  $\sim 0.4$  dex in the predicted Li abundance for Pleiades stars at  $T_{\text{eff}} = 5000$  K. The low confidence in the abundances of JP 296, 298, 415, and 489 does not allow a direct comparison of those abundances and the Li abundances from JFSS, yet some general observations can be made.

Potassium abundances are useful when analyzing Li because of the similarities in the 7699 Å K I and 6707 Å Li I transitions and atomic data, and because K is not depleted throughout the MS lifetime of the star, which remains a possibility for Li. As such, relative K abundances were derived for all nine stars and are plotted against  $T_{\text{eff}}$  in the left panel of Figure 6; an analogous plot for  $\log N(\text{Li})$  is given in the right panel, the Li abundances for which were taken from JFSS. The similar behavior seen in these plots suggests that a portion of the observed Li depletion in cool dwarfs may be due to the same mechanism causing the trend in the K- $T_{\text{eff}}$

plane. Indeed, the derived M34 Li abundances generally lie below standard LTE model Li depletion predictions (Fig. 3 of JFSS). Linear approximations to the K- $T_{\text{eff}}$  and Li- $T_{\text{eff}}$  relations were made using the least-squares method, and the calculated slopes were compared. The K slope is  $\sim 60\%$  of the Li slope, pointing to the possibility that the cooler M34 Li abundances are systematically low. Attempting to eliminate this effect to first order, we have assumed that the warmest star in our sample has the characteristic cluster K abundance ( $[\text{K}/\text{H}] \sim 0.34$ ). Fitted K abundances were then calculated using the effective temperatures from JFSS and the linear approximation to the K- $T_{\text{eff}}$  relation. Star-to-star differences of the adopted cluster K abundance and the fitted K abundance were used to systematically raise the Li abundances. These modified Li abundances, along with the original JFSS Li abundances, are plotted as a function of  $T_{\text{eff}}$  in Figure 7. The solid lines are replicated standard model Li depletions from Figure 3 of JFSS. The modified Li abundances are generally higher than the model predictions, but this first-order approximation raises questions concerning the true slope of the Li depletion seen in cool cluster dwarfs and, in the case of M34, possibly eliminates the need for MS Li depletion to describe the general trends of the observed data.

Chi-square tests provide a greater than 99% confidence level that the spreads seen in Figure 4 are greater than statistically expected for all the elements except Ni and Si. Again, the spreads are mostly a result of the four anomalous stars, pointing to a possible relation between the scatter of the elements (whatever the cause) considered herein and the scatter seen in the Li abundances. To test this, polynomial fits were made to the  $[\log N(\text{Li})]-(B-V)_0$  and  $[\text{M}/\text{H}]-(B-V)_0$  data, where “M” here is Fe, Cr, Si, Al, Mg, and K. The differences in the observed and fitted abundances of Li are plotted against the same differences for M in Figure 8. No correlation is seen between the scatter of the elements studied here and that of Li. In addition, the fact that there is no scatter in the elements for the five warm stars from which the mean cluster abundances have been derived suggests that the intracluster Li dispersions seen in M34 are not correlated with star-to-star scatter of the elements. Wilden et al. (2002) found similar results in their recent study of the Pleiades.

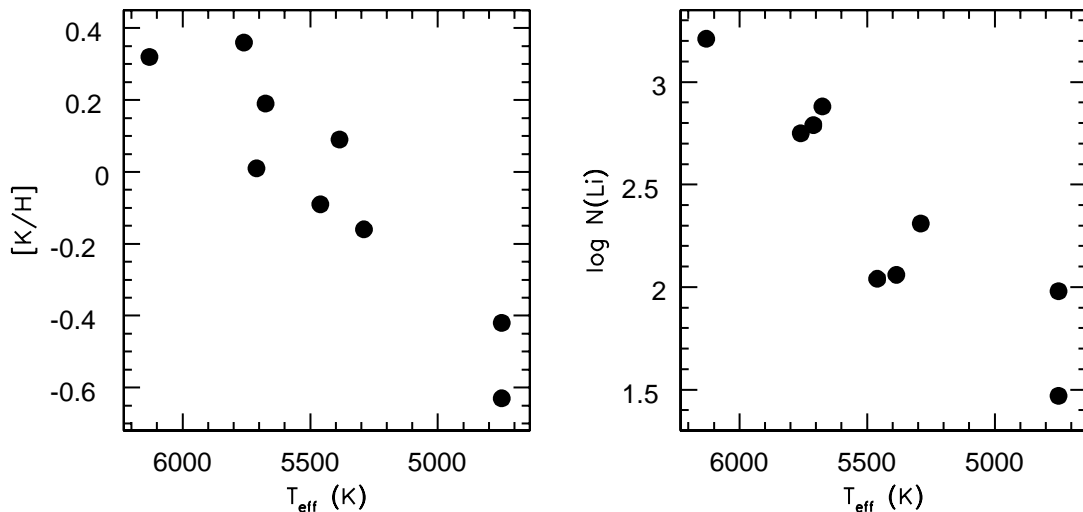


FIG. 6.— $[\text{K}/\text{H}]$  and  $\log N(\text{Li})$  plotted against  $T_{\text{eff}}$ . The Li abundances are taken from JFSS.

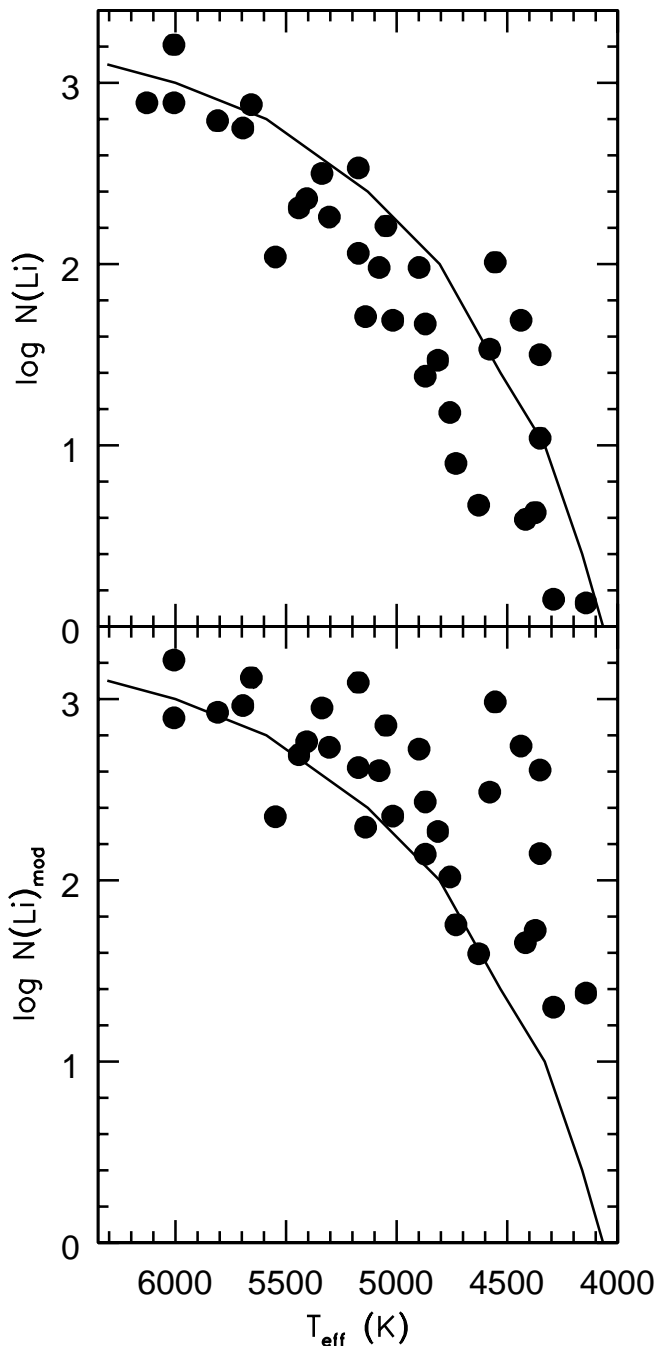


FIG. 7.—Li abundance as a function of  $T_{\text{eff}}$ . The solid lines are Li depletion predictions as seen in Fig. 3 of JFSS. The  $T_{\text{eff}}$ 's in both plots and the Li abundances in the top panel are those from JFSS. The Li abundances in the bottom panel are the modified JFSS abundances as described in the text.

## 6. SUMMARY

We have derived abundances for Fe, Ni, Ti, Cr, Ca, Si, Al, and Mg for nine G and K dwarfs in the open cluster M34 from high-resolution spectra obtained with the HIRES spectrograph on the Keck I Telescope. Accurate abundances of open cluster stars are important to modern astrophysics on many fronts, including determining the adequacy of stellar models, investigating the Li patterns seen in clusters such as M34 and the Pleiades, securing confidence in distances derived from main-sequence fitting, and constraining Galactic chemical evolution. We have chosen stars with

temperatures in the range  $4750 \text{ K} \leq T_{\text{eff}} \leq 6130 \text{ K}$  and with rotational velocities  $\leq 11 \text{ km s}^{-1}$ . Only those stars falling on or near the expected cluster MS and with high proper-motion membership probabilities were analyzed, with the exception of JP 296. This star is believed to be a member based on its position near the cluster MS, but its disparate radial velocity lies outside that for the cluster, suggesting it is a single-lined spectroscopic binary. Membership was assumed for JP 296.

Plotting the derived abundances as a function of  $T_{\text{eff}}$  revealed a small but statistically significant correlation for all the elements except Ni. The relations were such that the cool stars were found to have lower abundances than the warmer stars, the exception being Si, where the cooler stars were overabundant compared with the warmer stars. Comparing the abundances derived from Fe I and Fe II revealed a significant overionization in JP 296, 298, 415, and 489, four of the coolest stars of the study. The opposite correlation seen in the  $[\text{Si}/\text{H}]-T_{\text{eff}}$  plane is intriguing because of its differing excitation behavior compared with the other elements; its excitation potentials are higher. These observed relations implicate the action of NLTE mechanisms, though we cannot rule out systematic effects from the model atmospheres used. There has been one study that found doubt with respect to the Kurucz models' being applied to cool stars (Gratton et al. 1996), though that study found inadequacies for stars with  $T_{\text{eff}} \leq 4400 \text{ K}$ , cooler than the stars considered here. Whatever the cause, the derived abundances of the four stars are of low confidence and not included in the cluster means.

The final iron abundance derived from Fe I is  $0.07 \pm 0.04$  dex. The Ni underabundance with respect to Fe of  $-0.12 \pm 0.04$  dex lies on the outer boundary of the Edvardsson et al. (1993) field star data, similar to what was found for the two Pleiades K dwarfs of King et al. (2000). The rest of the elemental abundances are unremarkable compared with the field star data of Edvardsson et al. and are generally solar. Chromium is the only element for which a spread in the derived abundances is greater than statistically expected. We place an upper limit on the Cr scatter of 0.09 dex.

The study of M34 would be greatly benefited in several ways by more high-quality data. First, and possibly most importantly, is the possible overionization real or is it a product of the inability of model atmospheres to correctly predict the abundances of cool stars? A broader wavelength coverage would provide ionized lines of other elements, which can be used to corroborate the observed Fe overionization. Second, if NLTE effects are present in only selected cool stars, is there a correlation to the Li depletion seen among this group? A comparison of the Li and K trends with  $T_{\text{eff}}$  suggests that the Li depletion in cool M34 stars may partially be due to mechanisms other than MS depletion. However, the Li scatter seems not to be related to the scatter of the other elements, suggesting that the Li scatter is not due to intracluster abundance variations. A greater understanding and treatment of NLTE in cool solar-type dwarfs is needed in regard to the depletion and scatter patterns; more data from cool dwarfs ( $< 5400 \text{ K}$ ) will help in this analysis. Third, is the  $[\text{Ni}/\text{Fe}]$  underabundance real? A larger sample of stars would help pinpoint the Ni abundance. Fourth, more data are needed in order to solidify the abundances of all the elements. The cluster mean abundance of any element needs a statistically significant number of stars before it can be stated with true confidence.

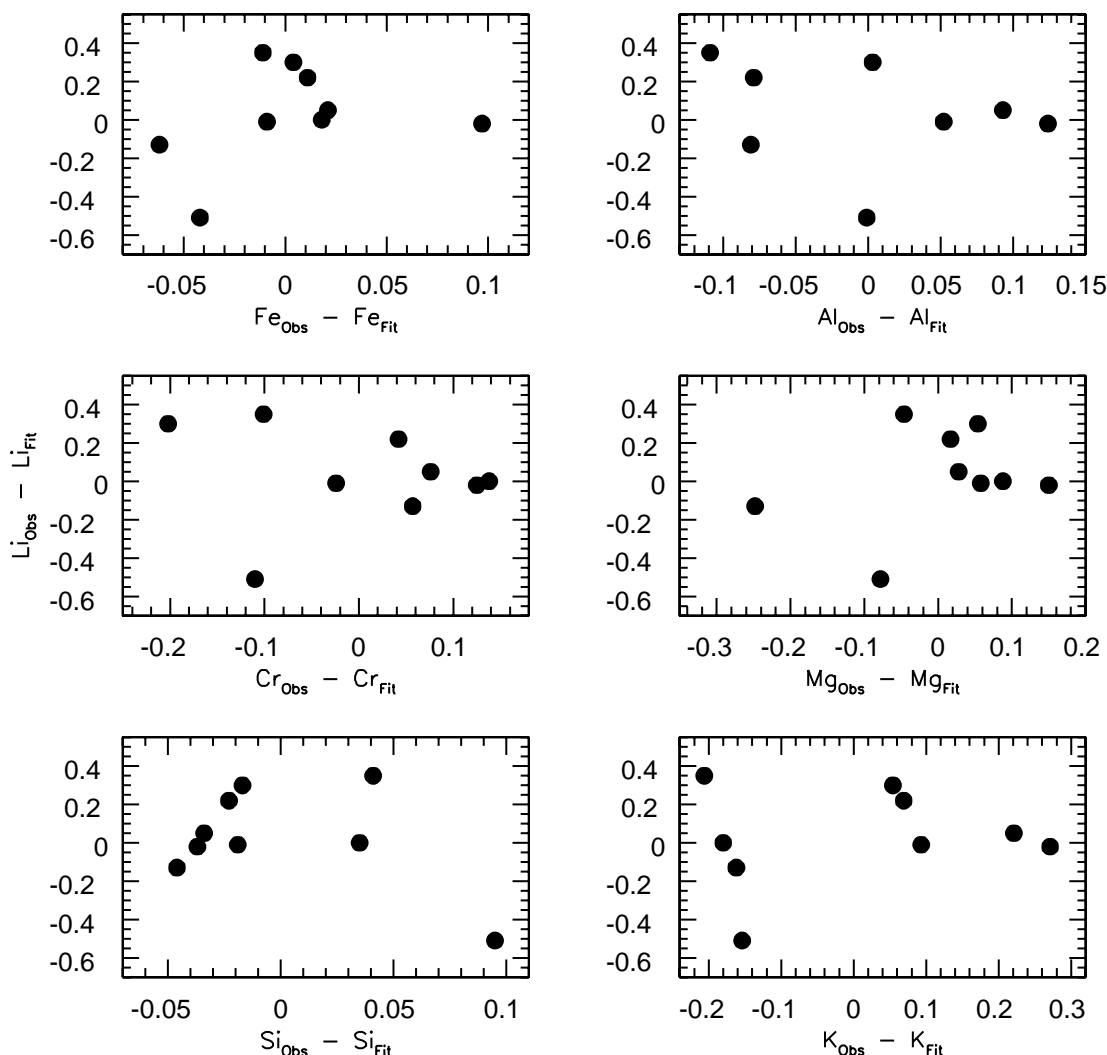


FIG. 8.—Observed and fitted Li abundance differences vs. observed and fitted metal abundance differences. The fitted abundances are those calculated using a polynomial fit to the  $N(\text{Li})-(B-V)_0$  and  $[\text{M}/\text{H}]-(B-V)_0$  relations.

S. C. S. and J. R. K. gratefully acknowledge support for this work provided by grant AST 00-86576 to J. R. K. from the National Science Foundation. B. F. J. gratefully acknowledges support for this work from NSF grant AST 99-88105. The observations were made at the W. M. Keck Observatory, which is operated as a scientific partnership among the California Institute of Technology, the University

of California, and the National Aeronautics and Space Administration. The Observatory was made possible by the generous financial support of the W. M. Keck Foundation. This research has made extensive use of NASA's Astrophysics Data System. We would like to thank C. Deliyannis and A. Steinhauer for sharing WIYN Open Cluster Study preliminary M34 results and other insights with us.

#### REFERENCES

- Barrado y Navascués, D., Deliyannis, C. P., & Stauffer, J. R. 2001, *ApJ*, 549, 452  
 Boesgaard, A. M. 1989, *ApJ*, 336, 798  
 Boesgaard, A. M., & Friel, E. D. 1990, *ApJ*, 351, 467  
 Canterna, R., Perry, C. L., & Crawford, D. L. 1979, *PASP*, 91, 263  
 Cayrel, R., Cayrel de Strobel, G., & Campbell, B. 1985, *A&A*, 146, 249  
 Chaboyer, B., Demarque, P., & Pinsonneault, M. H. 1995, *ApJ*, 441, 876  
 Duncan, D. K., & Jones, B. F. 1983, *ApJ*, 271, 663  
 Edvardsson, B., Andersen, J., Gustafsson, B., Lambert, D. L., Nissen, P. E., & Tomkin, J. 1993, *A&A*, 275, 101  
 Feltzing, S., & Gustafsson, B. 1998, *A&AS*, 129, 237  
 Fernandes, J., Lebreton, Y., Baglin, A., & Morel, P. 1998, *A&A*, 338, 455  
 Fitzpatrick, M. J., & Sneden, C. 1987, *BAAS*, 19, 1129  
 García López, R. J., Rebolo, R., Herrero, A., & Beckman, J. E. 1993, *ApJ*, 412, 173  
 Gehren, T., Korn, A. J., & Shi, J. 2001, *A&A*, 380, 645  
 Gonzalez, G., Laws, C., Tyagi, S., & Reddy, B. E. 2001, *AJ*, 121, 432  
 Gratton, R. G., Carretta, E., & Castelli, F. 1996, *A&A*, 314, 191  
 Gray, D. F. 1992, *The Observation and Analysis of Stellar Photospheres* (2d ed.; Cambridge: Cambridge Univ. Press)  
 Ianna, P. A., & Schlemmer, D. M. 1993, *AJ*, 105, 209  
 Jones, B. F., Fischer, D., Shetrone, M., & Soderblom, D. R. 1997, *AJ*, 114, 352 (JFSS)  
 Jones, B. F., & Prosser, C. F. 1996, *AJ*, 111, 1193 (JP)  
 King, J. R. 1993, Ph.D. thesis, Univ. Hawaii  
 King, J. R., & Hiltgen, D. D. 1996, *AJ*, 112, 2650  
 King, J. R., Soderblom, D. R., Fischer, D., & Jones, B. F. 2000, *ApJ*, 533, 944  
 Kurucz, R. L., Furenlid, I., Brault, J., & Testerman, L. 1984, *Solar Flux Atlas from 296 to 1300 nm* (Sunspot, NM: Natl. Sol. Obs.)

- Piau, L., & Turck-Chièze, S. 2002, *ApJ*, 566, 419
- Pinsonneault, M. H., Stauffer, J., Soderblom, D. R., King, J. R., & Hanson, R. B. 1998, *ApJ*, 504, 170
- Robichon, N., Arenou, F., Mermilliod, J.-C., & Turon, C. 1999, *A&A*, 345, 471
- Snedden, C. 1973, *ApJ*, 184, 839
- Soderblom, D. R., Jones, B. F., Balachandran, S., Stauffer, J. R., Duncan, D. K., Fedele, S. B., & Hudon, J. D. 1993, *AJ*, 106, 1059
- Swenson, F. J., Faulkner, J., Rogers, F. J., & Iglesias, C. A. 1994, *ApJ*, 425, 286
- Thévenin, F. 1990, *A&AS*, 82, 179
- Thévenin, F., & Idiart, T. P. 1999, *ApJ*, 521, 753
- Thorburn, J. A., Hobbs, L. M., Deliyannis, C. P., & Pinsonneault, M. H. 1993, *ApJ*, 415, 150
- Thorén, P., & Feltzing, S. 2000, *A&A*, 363, 692
- VandenBerg, D. A., & Bridges, T. J. 1984, *ApJ*, 278, 679
- Vogt, S. S. 1992, in *ESO Workshop on High Resolution Spectroscopy with the VLT*, ed. M-H. Ulrich (Garching: ESO), 223
- Wilden, B. S., Jones, B. F., Lin, D. N. C., & Soderblom, D. R. 2002, *AJ*, 124, 2799